Nano-Related Effects

1. Switching
2. Motors
3. Sensing
4. Percolation
5. Actuators
6. Quantum effects
7. Energy conversion
8. Energy storage
9. controlled uptake & release
10. Self cleaning
11. Self assembly
12. Proximity effects

Nano Composites

Super tough & super hard – grain boundary engineering: Co/WC, Al/Al_2O_3

- CREEP AND WEARE RESISTANCE
- INCREASE OF BEND STRENGTH
- INCREASE OF FRACTURE TOUGHNESS

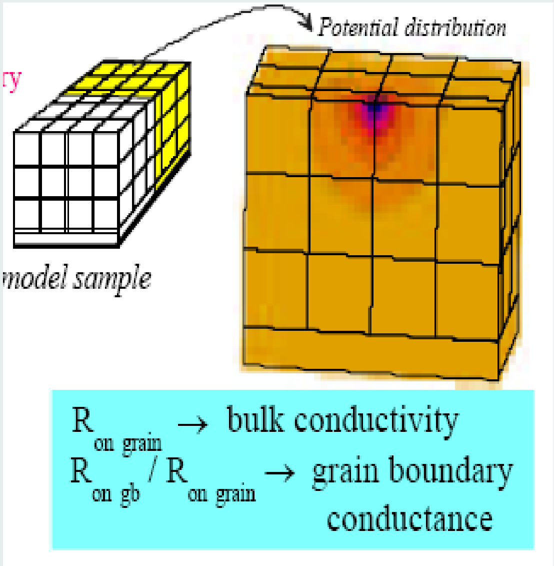

Many grain boundaries ➔ low heat conductivity

Many grain boundaries ➔ high ionic conductivity

Optimal ceramic filling rate

Samurai & Damazene Swords

Nano shaping of steels

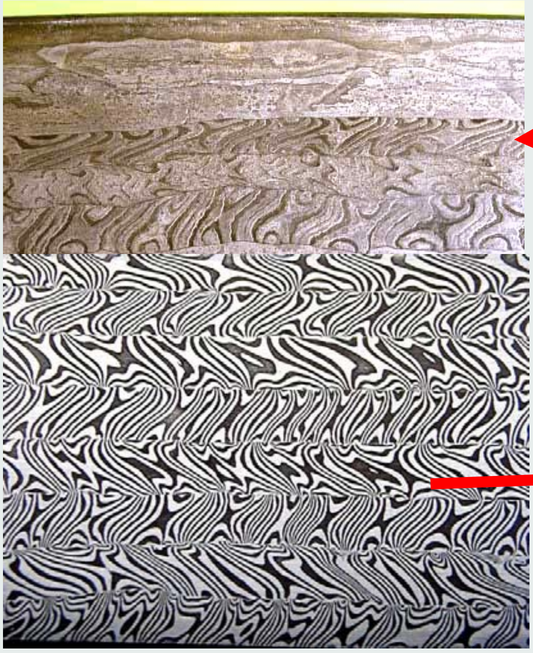

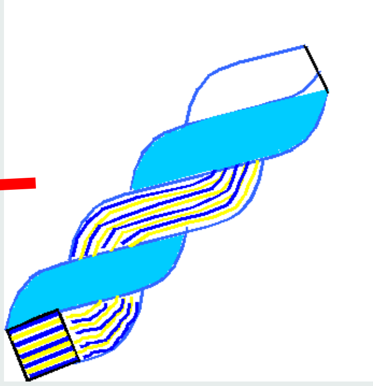

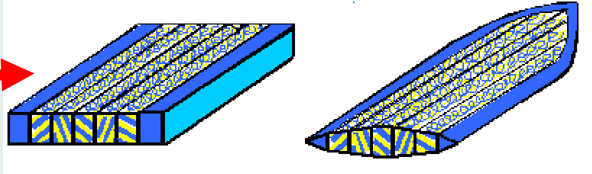

Phonon Engineering

Scattering on lattice vibrations is the most fundamental impairment to the performance of high speed electronic and optoelectronic devices.

Spatial confinement of phonons in nanostructures can strongly affect the phonon spectrum and modify phonon properties such as phonon group velocity, polarization, density of states and electron - phonon interaction.

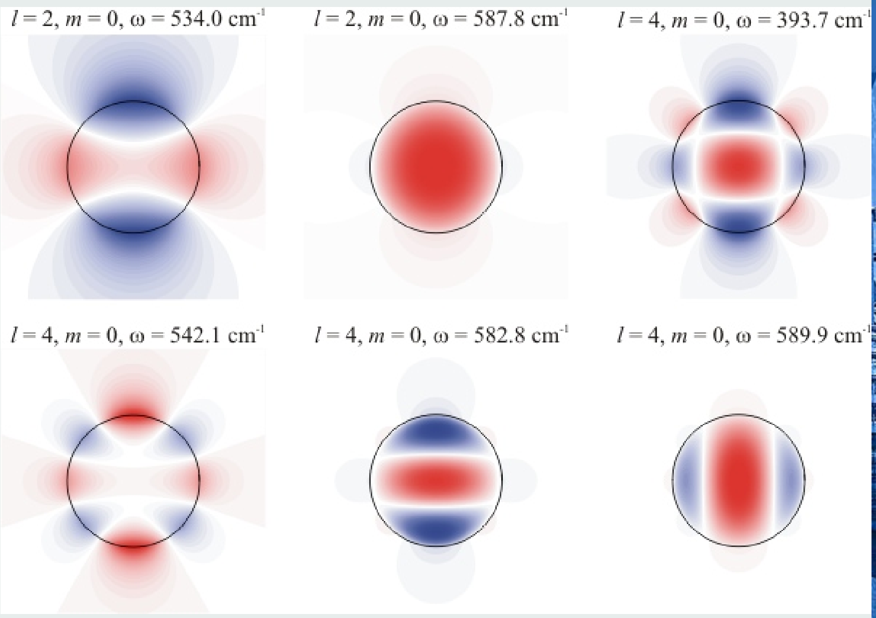

Quantum Antidots

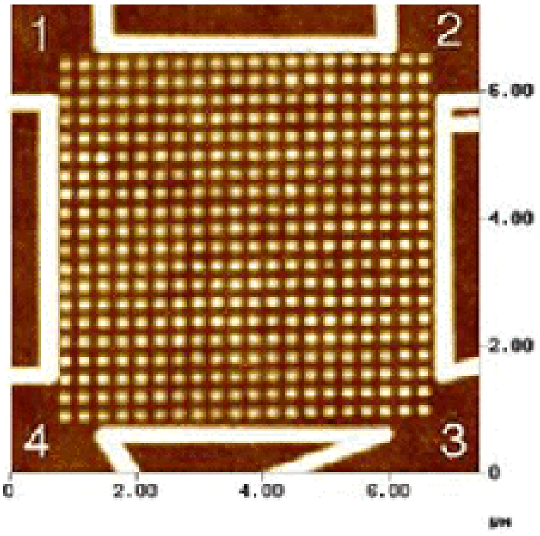

Electron micrograph of an antidot lattice [from K. Ensslin, ETH Zürich]. The lattice is a periodic array of holes "drilled" in a two-dimensional electron gas.

Electrons traveling through the lattice essentially behave as classical billard balls that experience random kicks at the holes.

However, at subkelvin temperatures the wave nature of the electron becomes important. In this regime one finds periodic oscillations in the magnetotransport through the antidot lattices.

Molecular Magnets

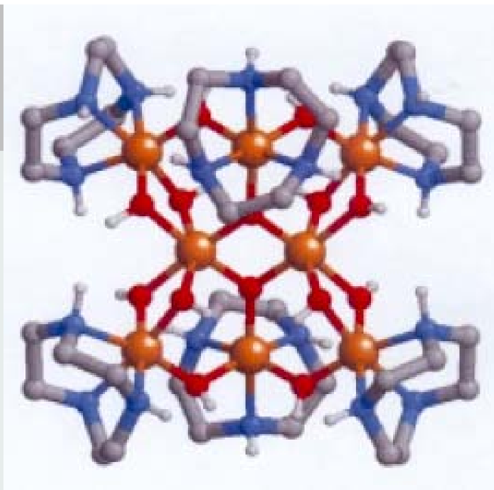

Molecular magnets are systems where a permanent magnetization and magnetic hysteresis can be achieved (although usually at extremely low temperatures) not through a three-dimensional magnetic ordering, but as a purely one-molecule phenomenon.

The requisites for such a system are:
a high spin ground state
a high zero-field-splitting (due to high magnetic anisotropy)

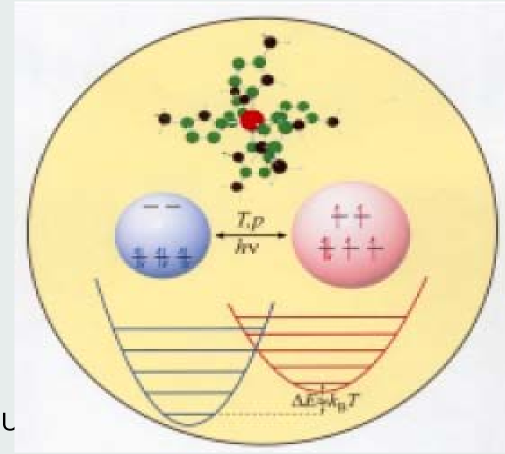

Molecular Machines

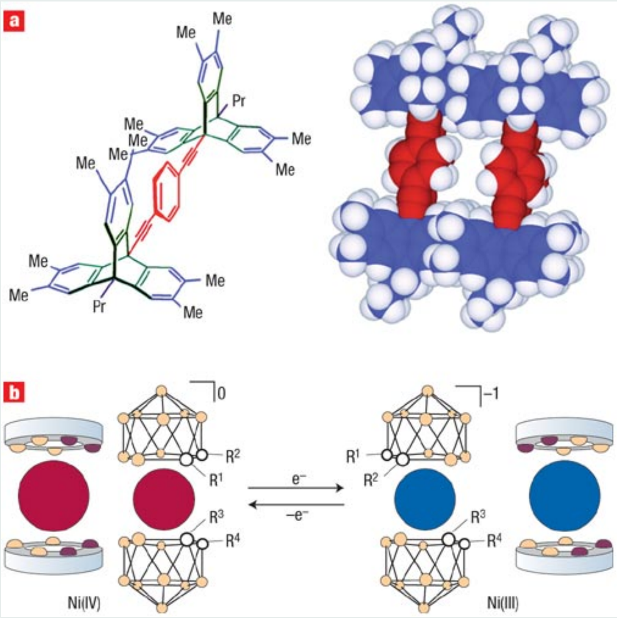

Examples of non-directionally controlled molecular rotors. a, A molecular rotor (left) where hindrance to rotation of the central phenyl ring (the rotor) is removed by the upper and lower bulky molecular end units (the stators). Sufficient spacing for the phenyl rings is generated to allow fast rotation in the solid state as illustrated for two rotor units (right).

b, An electrochemically driven rotor where the upper and lower carborane (polyhedral clusters comprising boron and carbon atoms) moieties are bound as ligands to a nickel ion functioning as a 'ball-bearing'. Oxidation and reduction of the nickel centre (the Ni3+ / Ni4+ redox cycle) leads to rotation of the upper ligand relative to the lower ligand, changing the relative position of the alkyl groups (R1–4) attached to the carborane ligands.

Molecular Machines

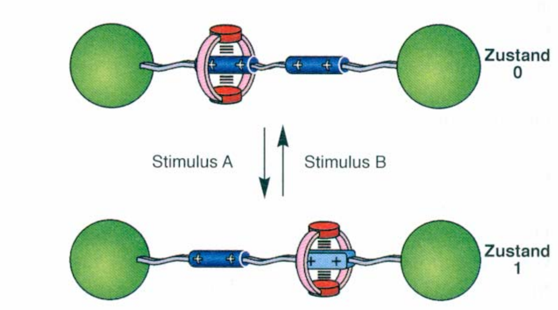

Redox switching

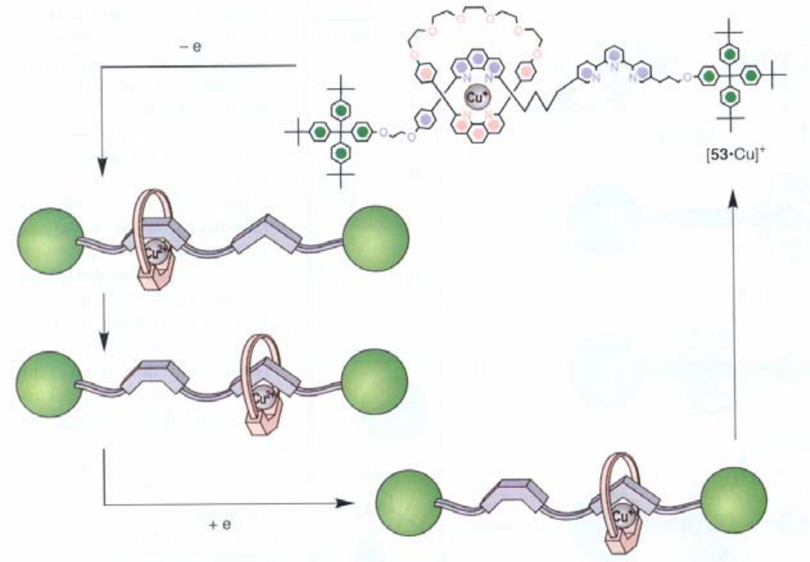

Molecular Valves

Two approaches to the opening and closing of nanovalves using molecular switches. a, A light-actuated nanovalve based on a mechano-sensitive channel protein modified with spiropyran photoswitches. When ultraviolet light is shone on the protein, the molecular switch is converted from its neutral, hydrophobic, form to a charged polar form. The change in hydrophobicity in the channel results in the channel opening. Visible light reverses the process and closes the channel again.
b, Photochemical allosteric control of a glutamatesensitive protein channel based on the azobenzene molecular switch. The switching unit is not incorporated in the channel itself but instead is located on the outside of the channel protein. Light of different color switches the system forth and back.

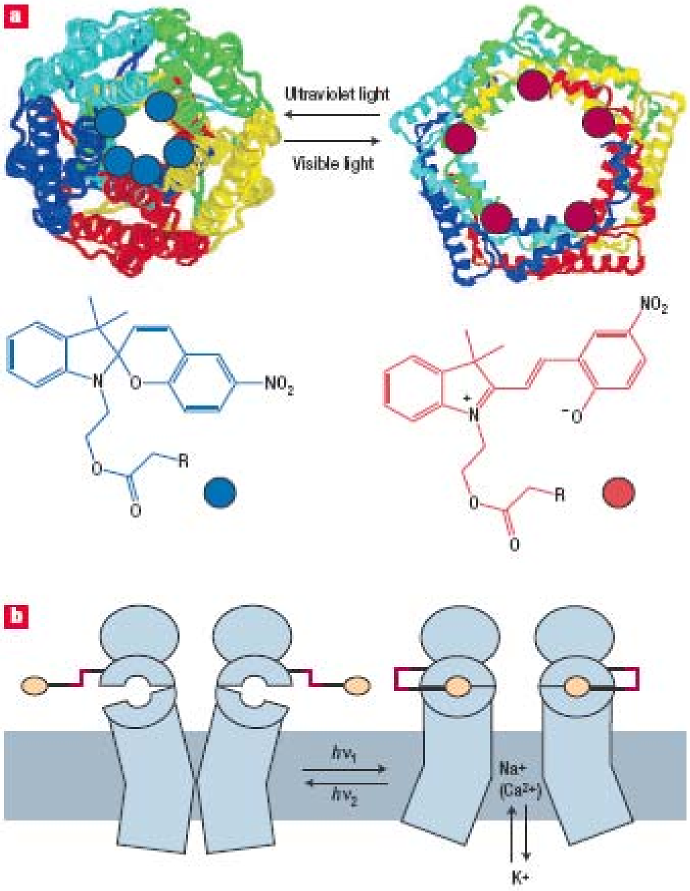

Brownian Rachet

http://monet.unibas.ch/~elmer/bm/

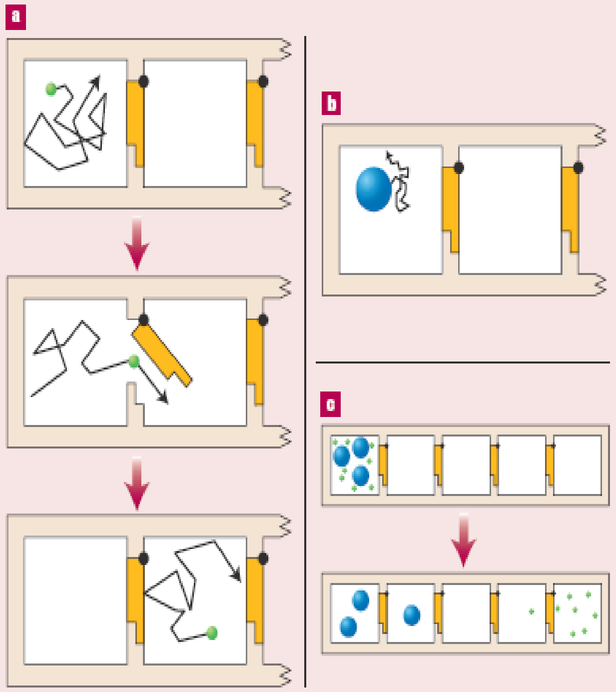

The Brownian ratchet exploits particle diffusion by using a series of gated compartments. In part a of the figure, a small particle (green) diffuses in a compartment until it hits a one-way gate that is controlled by a spring-loaded hinge. If the collision is sufficiently energetic, the gate opens instantaneously and allows the particle to pass into the next compartment.The one-way gate prevents the return of the particle to the previous compartment. In part b,a larger particle (blue) diffuses more slowly and has a much lower probability of hitting the gate with enough force to enter the next compartment. In this example,the asymmetry (a critical element of Brownian ratchets) is the different behaviour of the two particle types within the same type of compartment.By starting with a mixture of small and large particles (see c),the two types will separate over time.Eventually,all or nearly all of the small particles will end up in the last compartment while very few of the large particles will move at all.

Hard Magnets

Superparamagnets – Spin valves, reading heads

Ferrofluids – contactless heating, gaskets, protein separation

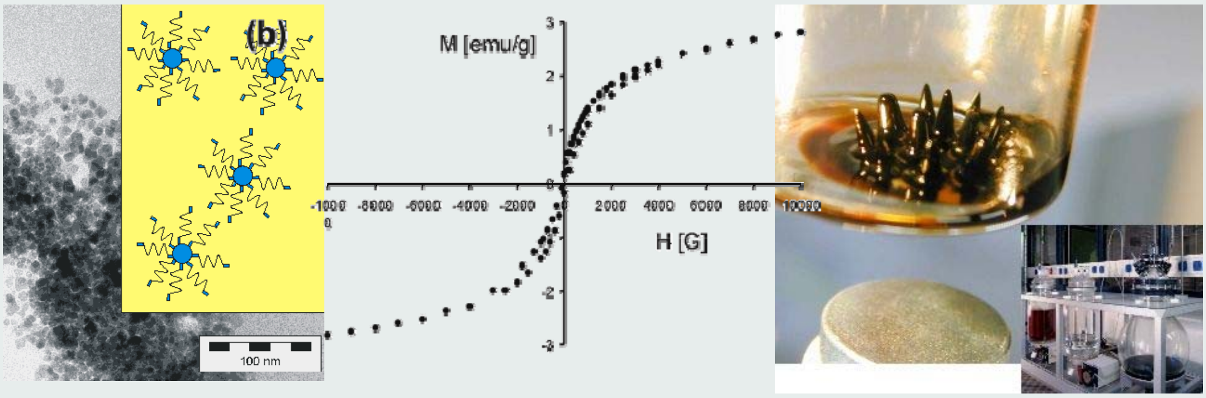

permanent magnets - < 30nm ➔ magnet drives

Size and Stability

Clausius-Clapeyron: size dependency of phase transition temperature

$$\frac{dP}{dT} = \frac{L}{T\Delta V}$$

where dP/dT is the slope of the coexistence curve, L is the latent heat, T is the temperature, and ΔV is the volume change of the phase transition.

Optimal size (Alivisatos) – largest hysteresis of phase transformation for nano size

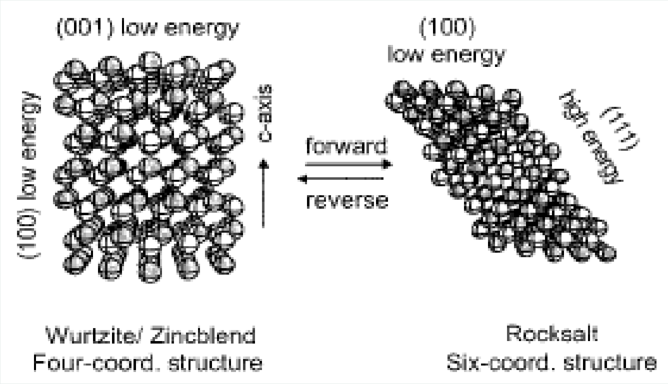

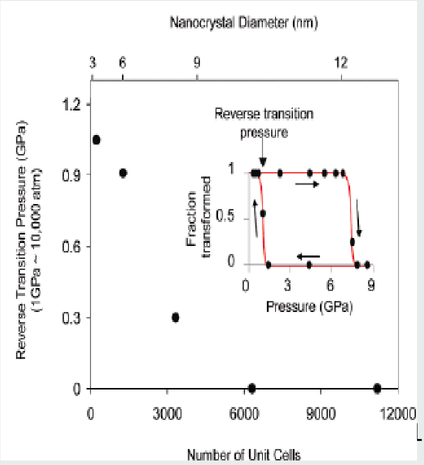

Quantum Size Effects in Metals

Size induced metal –insulator transition (SIMIT)

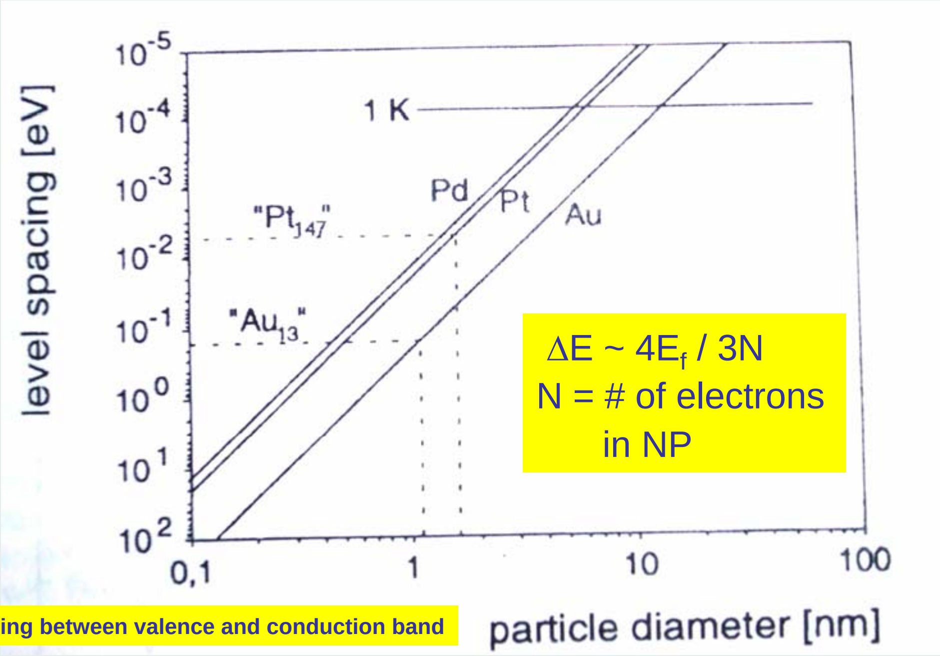

$\Delta E \sim 4E_f / 3N$
N = # of electrons in NP

ΔE = average level splitting between valence and conduction band

---

Quantum Size Effects in Semiconductors

Size induced metal –insulator transition (SIMIT)

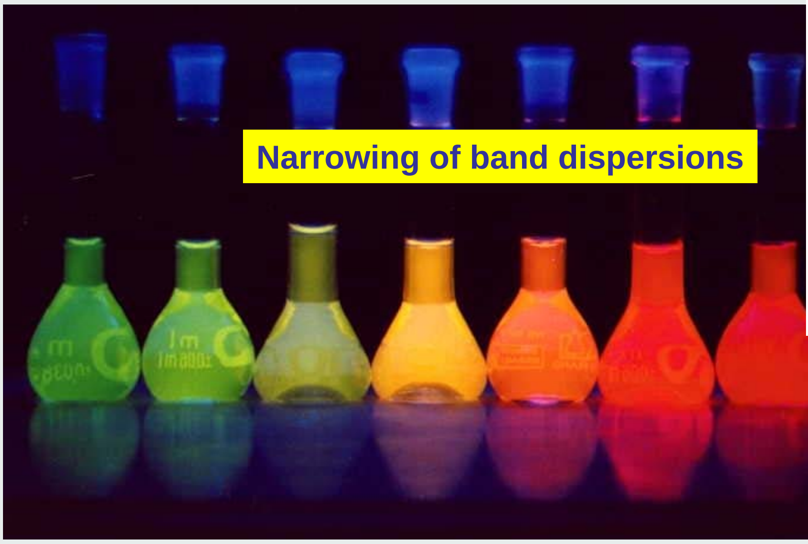

Narrowing of band dispersions

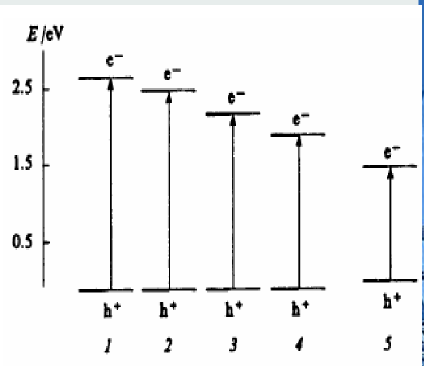

(1) 1nm
(2) 1.25nm
(3) 1.75nm
(4) 2nm
(5) bulk

← **Smaller particles**

Switchable Fermi Levels

Charge induced size change

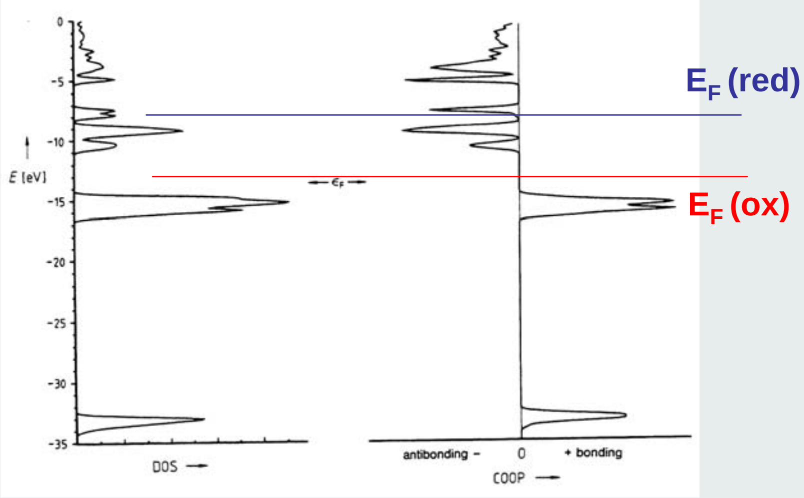

Enhanced Thermoelectricity

sharpening of the DOS towards smaller particle size

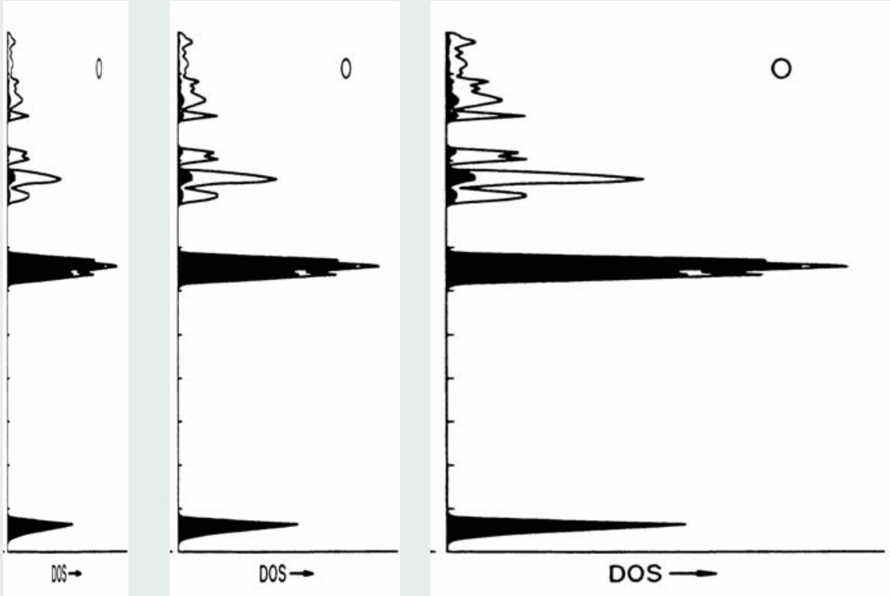

Proximity Effect

R. NESPER ETH ZÜRICH & COLLEGIUM HELVETICUM

Andreev reflection

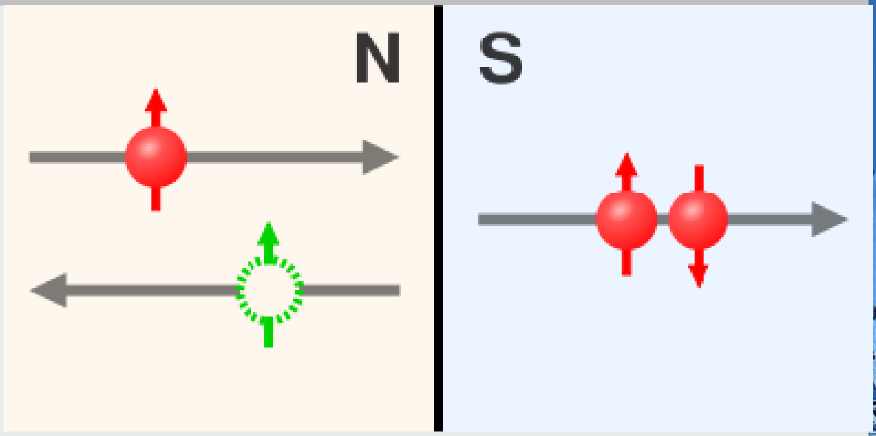

is a special type of particle scattering which occurs at interfaces between superconductors or superconductor-normal metal interfaces. In such a reflection process an electronic excitation incident on the interface is retro-reflected and converted into a hole and vice versa.

Photonic Surface Plasmons

R. NESPER ETH ZÜRICH & COLLEGIUM HELVETICUM

basis for a new type of photonics, one based on metallic materials rather than the traditional dielectric and semiconducting materials that dominate present day photonics technology. Metallic photonic materials demonstrate unique properties due to the existence on metals of electromagnetic surface waves known as surface plasmons. Surface plasmons are set to become part of the photonics revolution in which the interaction between light and matter is controlled by producing patterned structures that are periodic on the scale of the wavelength of light. Surface plasmons open up a wealth of new possibilities for photonics because they allow the concentration and propagation of light below the usual resolution limit, thus opening up such possibilities as sub-wavelength optical components.

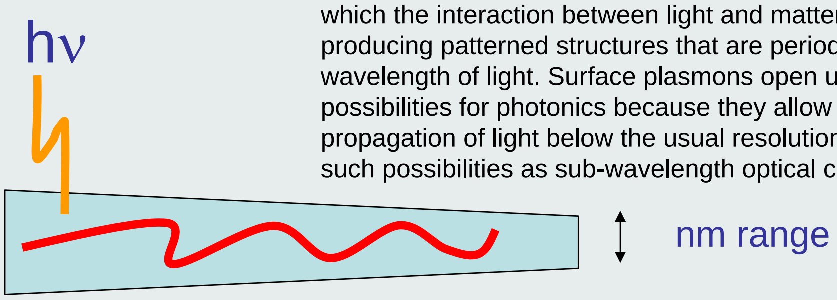

Light energy guiding below wave length threshold

Mie theory (1908), Vollmer&Kreibing 1995

20nm particles of Au, Ag, Cu have plasmon frequncies of 520nm, 380 nm and 560 nm

Selfassembly

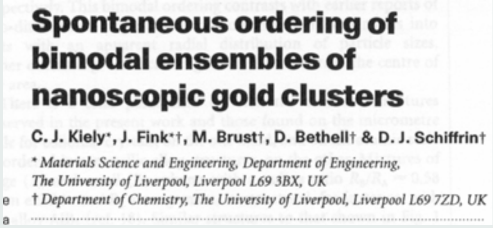

Spontaneous ordering of bimodal ensembles of nanoscopic gold clusters

C. J. Kiely*, J. Fink*†, M. Brust†, D. Bethell† & D. J. Schiffrin†

* *Materials Science and Engineering, Department of Engineering, The University of Liverpool, Liverpool L69 3BX, UK*
† *Department of Chemistry, The University of Liverpool, Liverpool L69 7ZD, UK*

Nature (1998) 396, 444

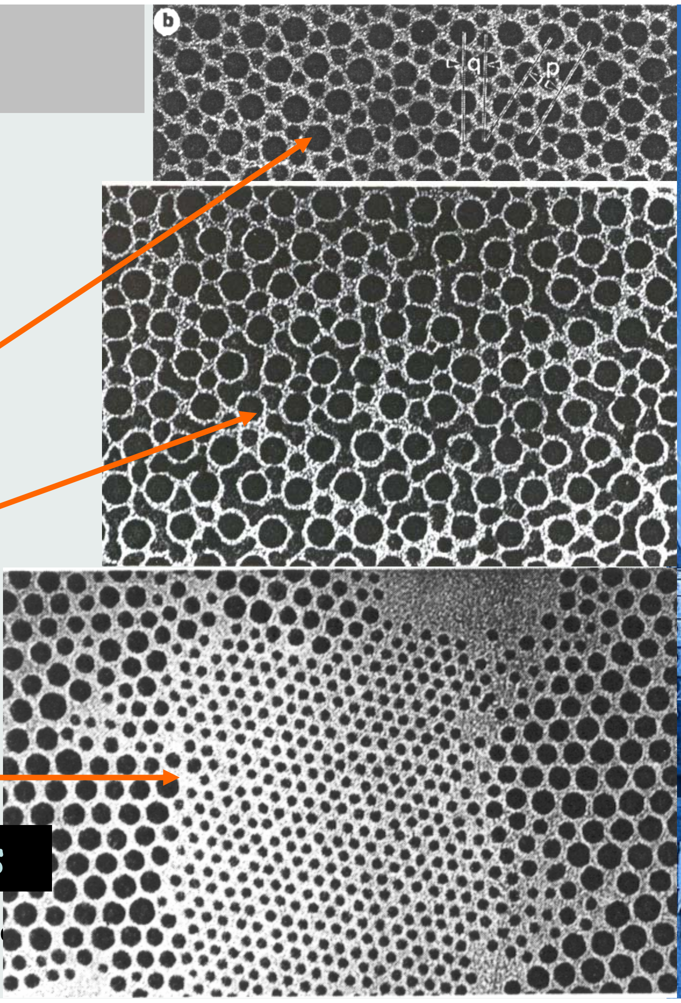

primary structure

after aging

phase separation

design – two cluster sizes

Alignment of anisotropic Nanoparticles

organic matrix / mould

Composite organic + α–FeOOH

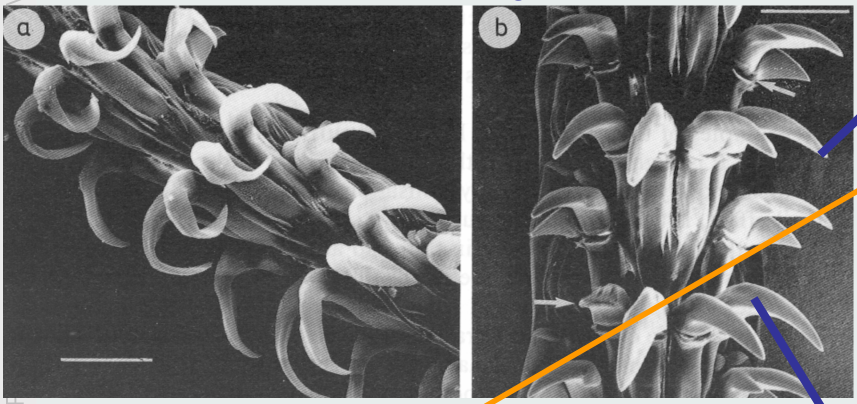

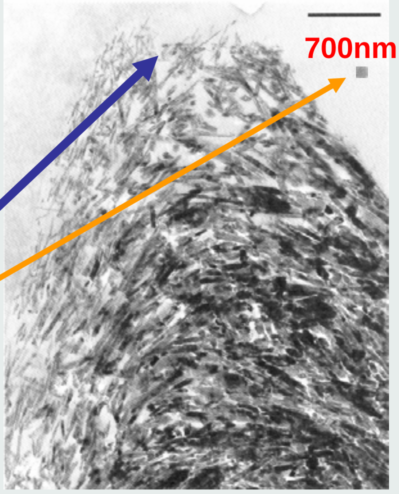

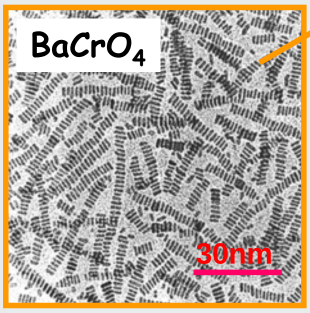

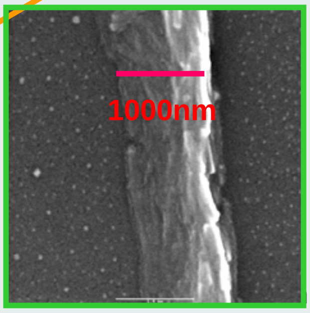

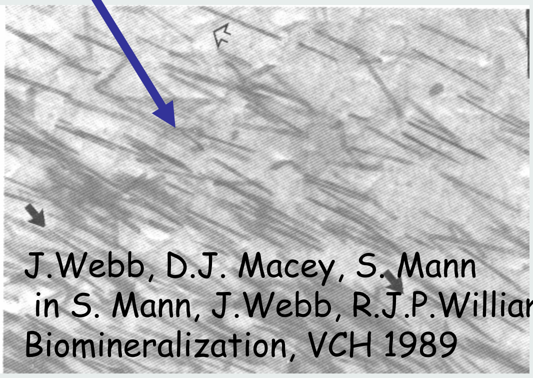

J.Webb, D.J. Macey, S. Mann
in S. Mann, J.Webb, R.J.P.Williams,
Biomineralization, VCH 1989

Silica - deep sea sponge

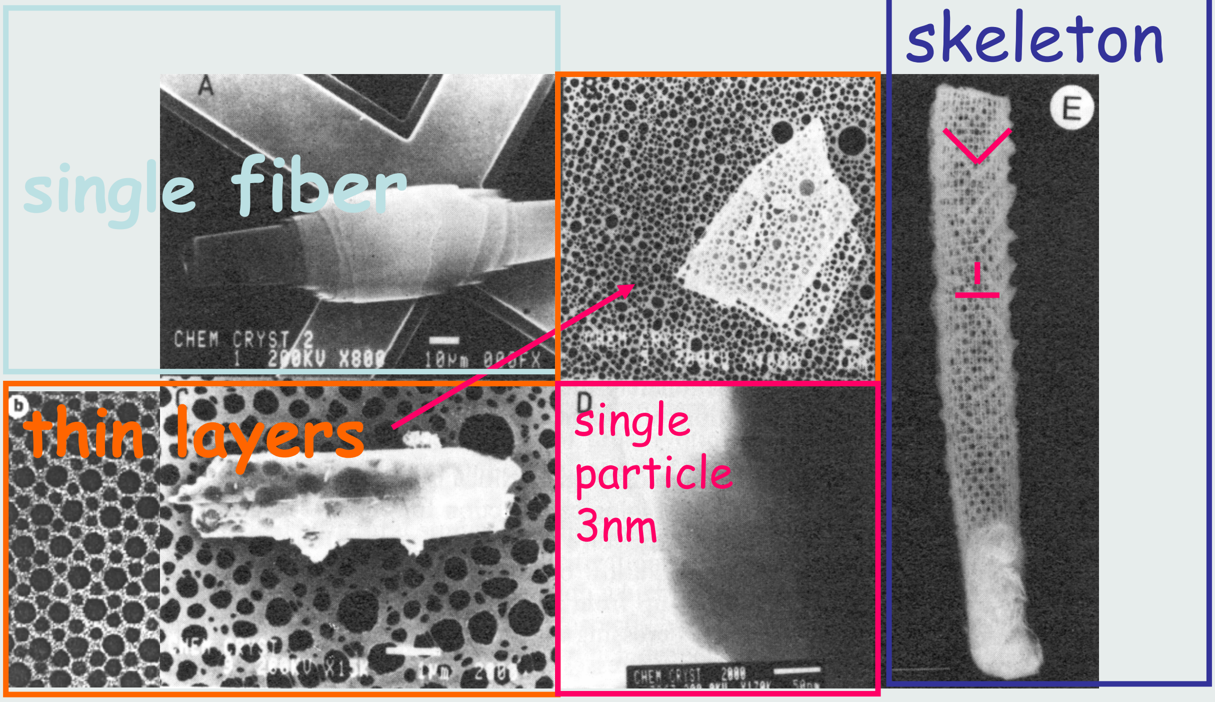

C.C.Perry in S. Mann, J.Webb, R.J.P.Williams, Biomineralization, VCH 1989

Bio-Mineralisation

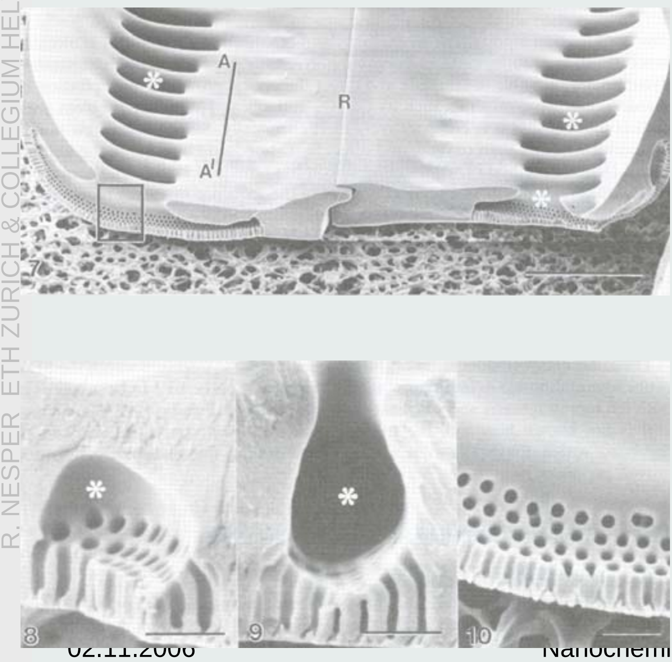

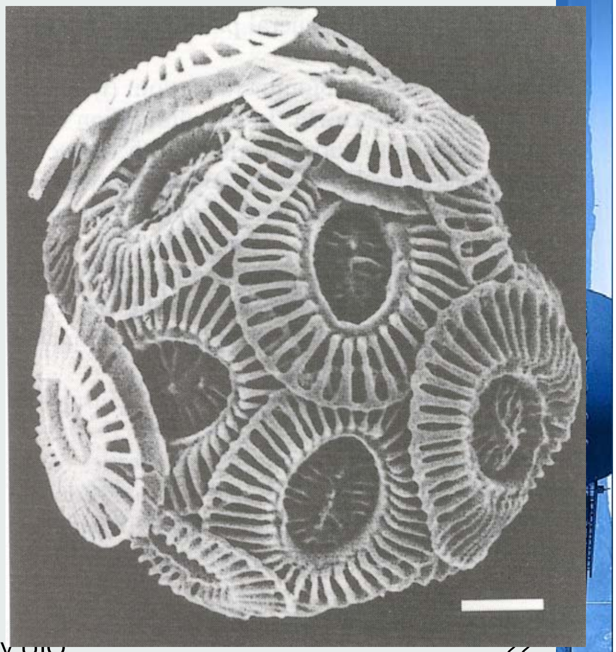

Vesicle networks

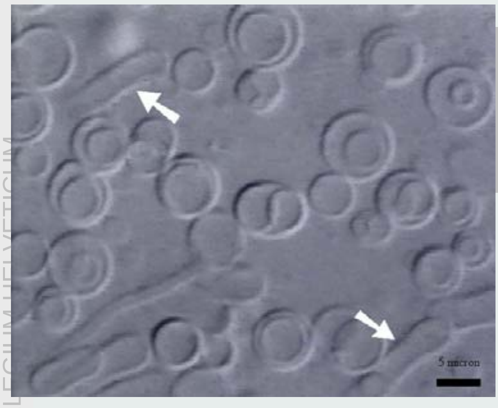

… in an observation period of 3 weeks 5 divisions have been observed …

- *very soft bonding*
- *slow and very sensible information system*

Solar Cell after M. Grätzel

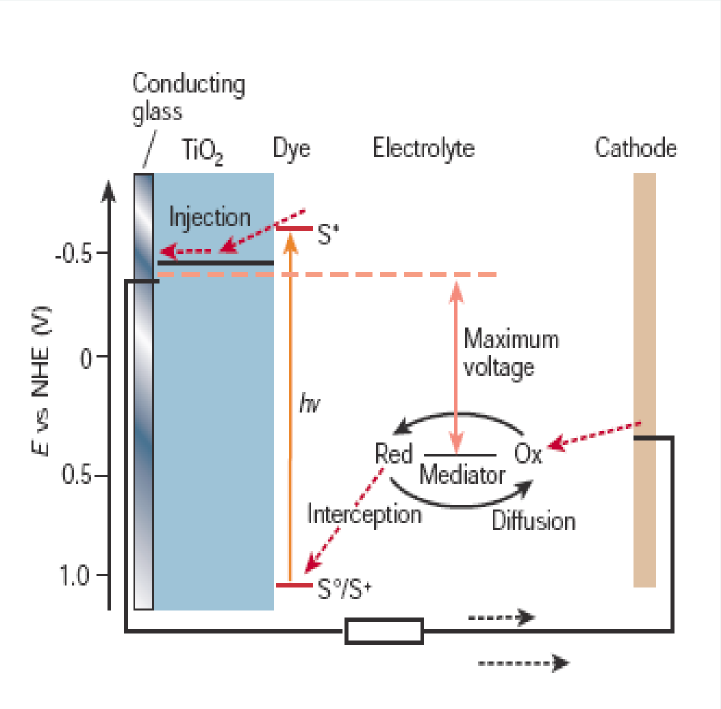

Tandem Cell for Water Cleavage

Based on two photosystems connected in series as shown in the electron flow diagram: A thin film of nanocrystalline tungsten trioxide, WO_3 (ref. 34), or Fe_2O_3 (ref. 35) serves as the top electrode absorbing the blue part of the solar spectrum. The valenceband holes (h+) created by band-gap excitation of the film oxidizewater to oxygen:

$$4h^+ + H_2O \Rightarrow O_2 + 4H^+$$

and the conduction-band electrons are fed into the second photosystem consisting of the dye-sensitized nanocrystalline TiO_2 cell discussed above. The latter is placed directly under the WO3 film, capturing the green and red part of the solar spectrum that is transmitted through the top electrode. The photovoltage generated by the second photosystem enables hydrogen to be generated by the conduction-band electrons.

$$4H^+ + 4e^- \Rightarrow 2H_2$$

The overall reaction corresponds to the splitting of water by visible light. There is close analogy to the 'Z-scheme' (named for the shape of the flow diagram) that operates in photosynthesis. In green plants, there are also two photosystems connected in series, one that oxidizes water to oxygen and the other generating the compound NADPH used in fixation of carbon dioxide.

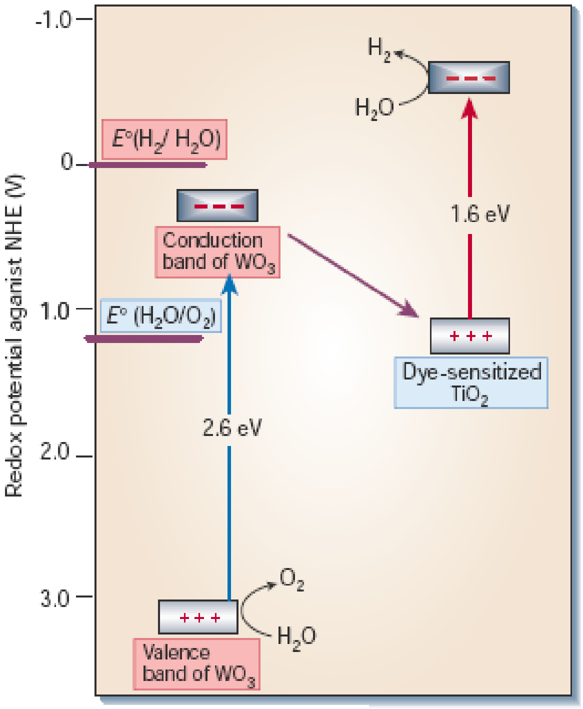

Grätzel, M. The artificial leaf, bio-mimetic photocatalysis. *Cattech* **3,** 3–17 (1999).

Present Solar Cells - Comparison

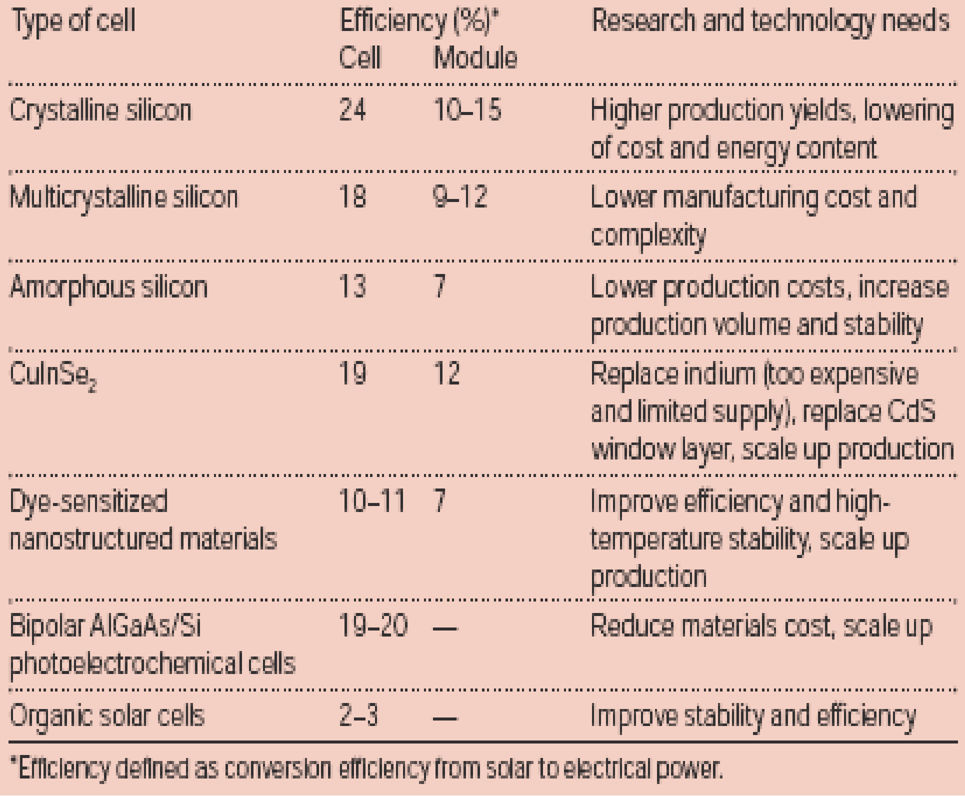

Type of cell	Efficiency (%)* Cell	Module	Research and technology needs
Crystalline silicon	24	10–15	Higher production yields, lowering of cost and energy content
Multicrystalline silicon	18	9–12	Lower manufacturing cost and complexity
Amorphous silicon	13	7	Lower production costs, increase production volume and stability
$CuInSe_2$	19	12	Replace indium (too expensive and limited supply), replace CdS window layer, scale up production
Dye-sensitized nanostructured materials	10–11	7	Improve efficiency and high-temperature stability, scale up production
Bipolar AlGaAs/Si photoelectrochemical cells	19–20	—	Reduce materials cost, scale up
Organic solar cells	2–3	—	Improve stability and efficiency

*Efficiency defined as conversion efficiency from solar to electrical power.

Continued Growth of CNTs

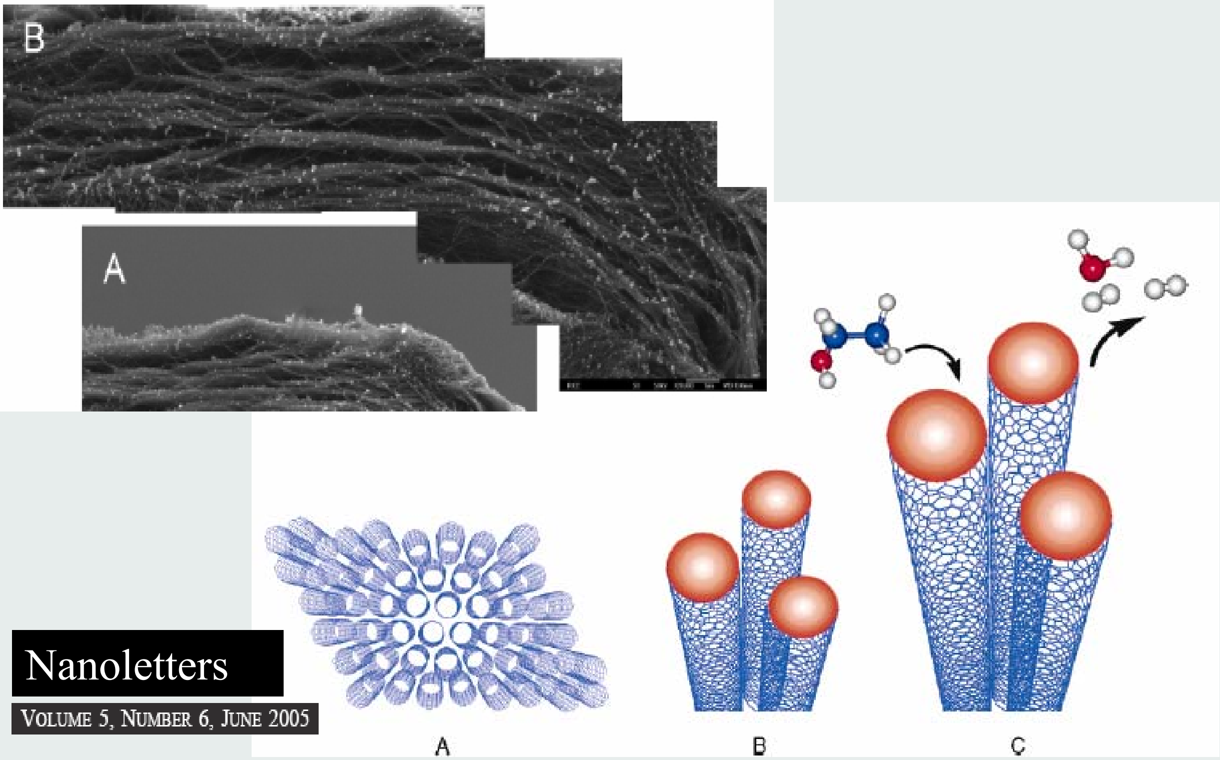

Nanoletters

Volume 5, Number 6, June 2005

Investigation of Grain Boundaries

Measurement principle

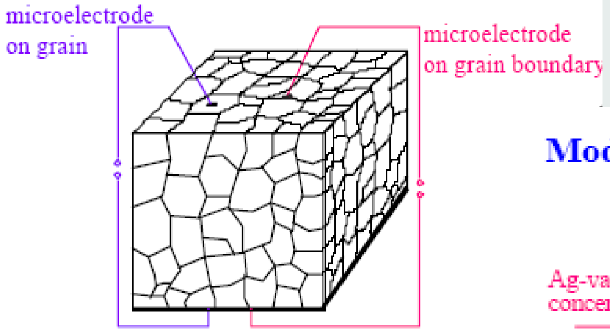

If $R_{\text{on grain}} > R_{\text{on gb}}$

→ grain boundary is highly conductive

Model: Space charge accumulation layer

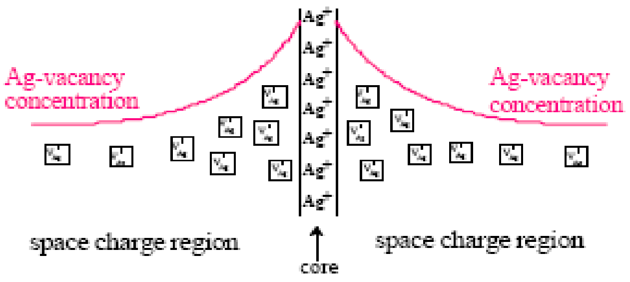

- Thickness of the conductive surface layer ≈ 4 µm
- Conductivity of the surface layer ≈ 100 x bulk conductivity
- enhanced conductivity due to mechanically induced grain boundaries

Single Crystal Growth

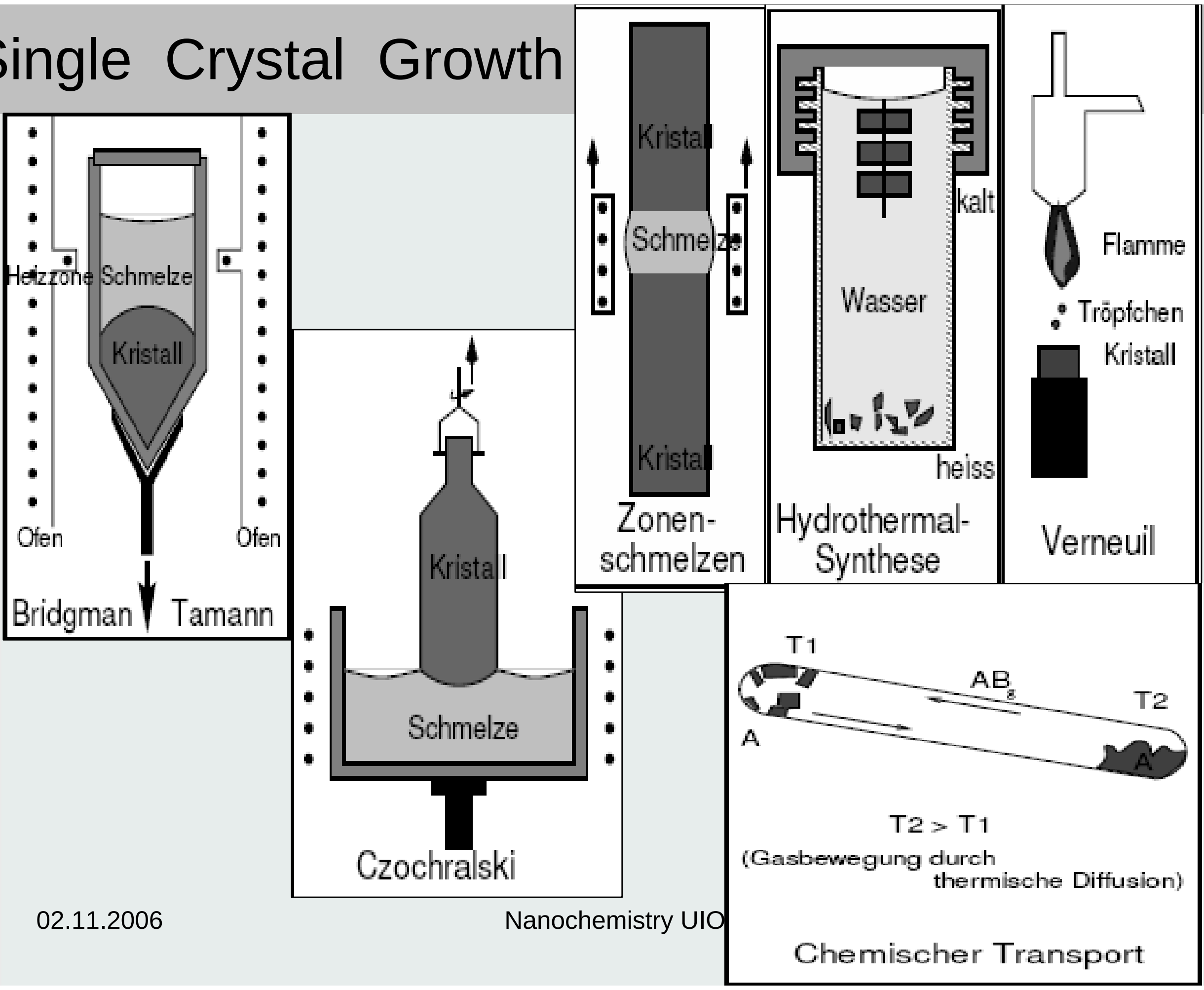

Battery with Porous Electrodes

Lithium ion-Battery

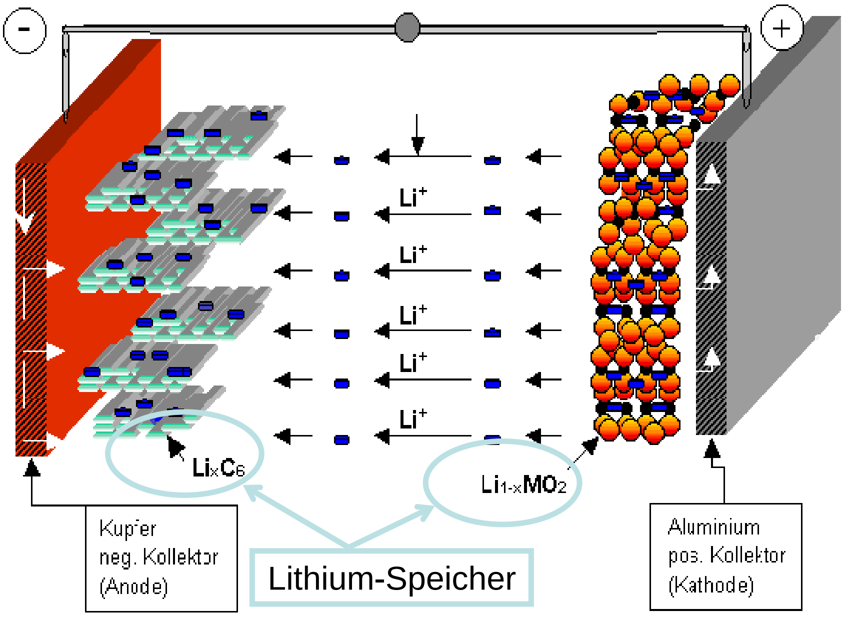

Batterien

R. NESPER ETH ZÜRICH & COLLEGIUM HELVETICUM

Charakterisierung elektrochemischer Zellen

Spezifische Ladung: $Q = zF/\sum_n M_n$ $\quad [\mathrm{Ah/kg}]$

$Q_v = Q \cdot \rho$ $\quad [\mathrm{Ah/l}]$ $\quad (\rho = \text{Dichte in kg/l})$

Spezifische Energie: $W = UQ = \dfrac{U \cdot z \cdot F}{\sum_n M_n} = -\dfrac{\Delta G}{\sum_n M_n}$ $\quad [\mathrm{Wh/kg}]$

Spezifische Leistung: $P = \dfrac{U \cdot i}{\sum_n m_n}$ $\quad [\mathrm{W/kg}]$

Batterien

R. NESPER ETH ZÜRICH & COLLEGIUM HELVETICUM

Ragone-Diagramm

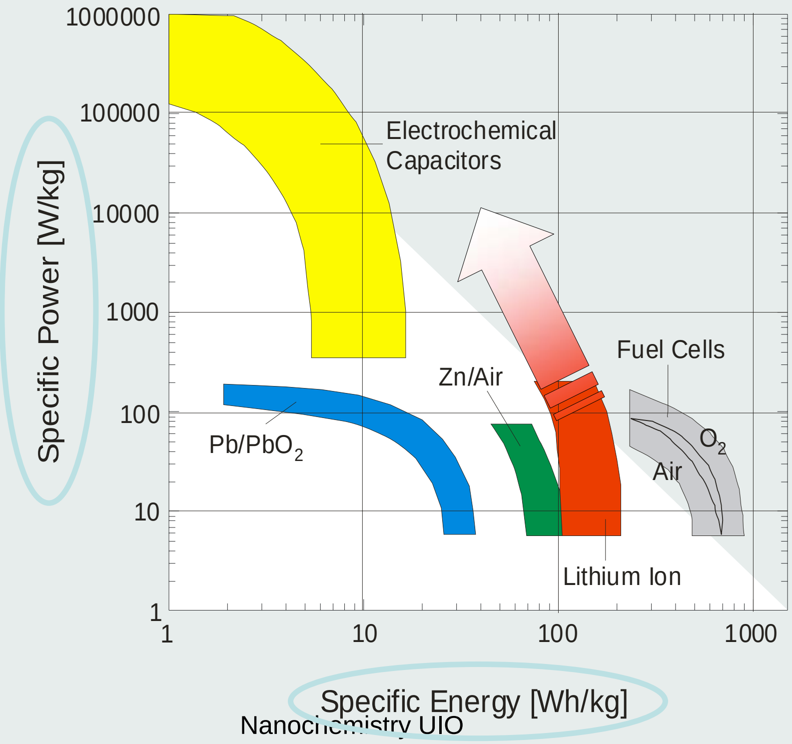

Batterien

Einige wichtige Batteriesysteme

	Anode (-)	Elektrolyt (Diaphragma)	Kathode (+)	
1.2 - 2 V Systeme wässerige Systeme	Pb	H_2SO_4	PbO_2	~ 30 - 50 Wh/kg
	Cd	KOH	NiOOH	
	MeH_x	KOH	NiOOH	~ 50 - 80 Wh/kg
	Zn	KOH	NiOOH	
	Zn	KOH	MnO_2	
	H_2	KOH	NiOOH	
	Zn	ZnBr, KBr	Br_2 - Komplex	
	Zn	KOH	O_2	~ 80 - 120 Wh/kg
2 - 4 V Systeme Aprotische Elektrolyte oder Festelektrolyte	Na	b-Al_2O_3	S_x	
	Na	b-Al_2O_3, $NaAlClO_4$	$NiCl_2$	
	Li	aprot. Lösungsmittel + Salz	MeO_x	
	Li	Polyäther + Salz	MeO_x	
	Li	Polyäther + Salz	Thio-org. Verb.	

Batterien

Lithiumionen-Batterie

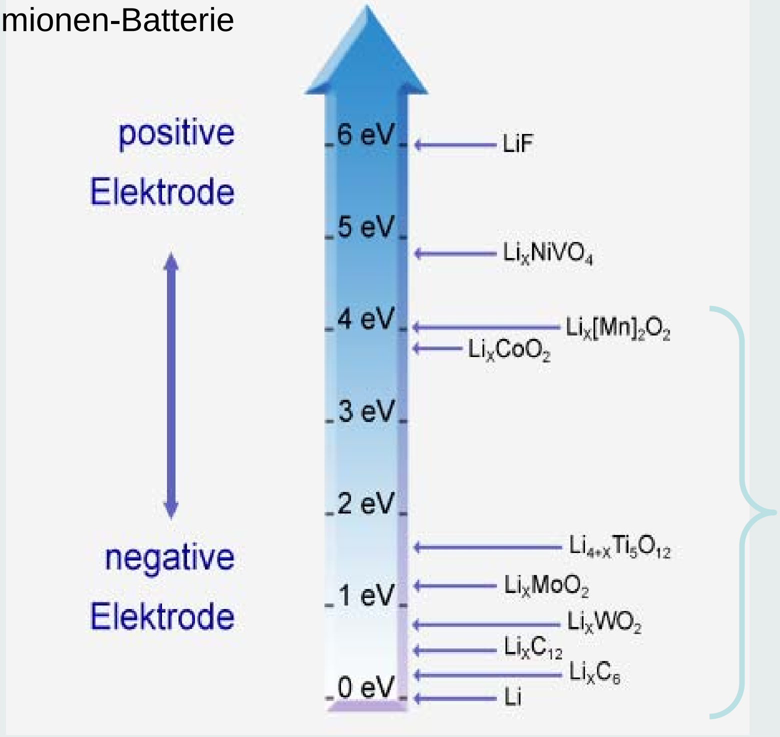

$$U = \Delta E \approx 4V$$

Elektrochemische Potentiale verschiedener Elektrodenmaterialien

Supercaps (Doppelschichtkondensatoren)

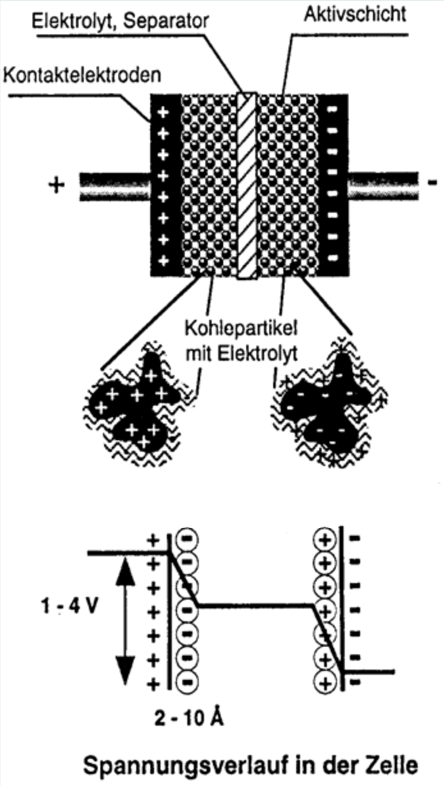

Spannungsverlauf in der Zelle

Elektrochemischer Doppelschichtkondensator

Energiedichte	$W_V = 1/2\ \varepsilon_0\ \varepsilon\ E^2$
E	5×10^7 V/cm
ε_0	8.8×10^{-14} F/cm
$\varepsilon_{\text{Doppelschicht}}$	ca. 10

Doppelschicht Kondensator mit 100 m^2/cm^3 — $W_V = 0.3$ kWh/l

➡ U = 1V — $W_V = 1.5$ Wh/l

➡ U = 4V — $W_V = 24$ Wh/l

Brennstoffzellen

- saure Brennstoffzellen
- alkalische Brennstoffzellen

- Niedertemperatur-Brennstoffzellen (100 °C)
- Mitteltemperatur-Brennstoffzellen (200 - 400 °C)
- Hochtemperatur-Brennstoffzellen (500 - 1000 °C)

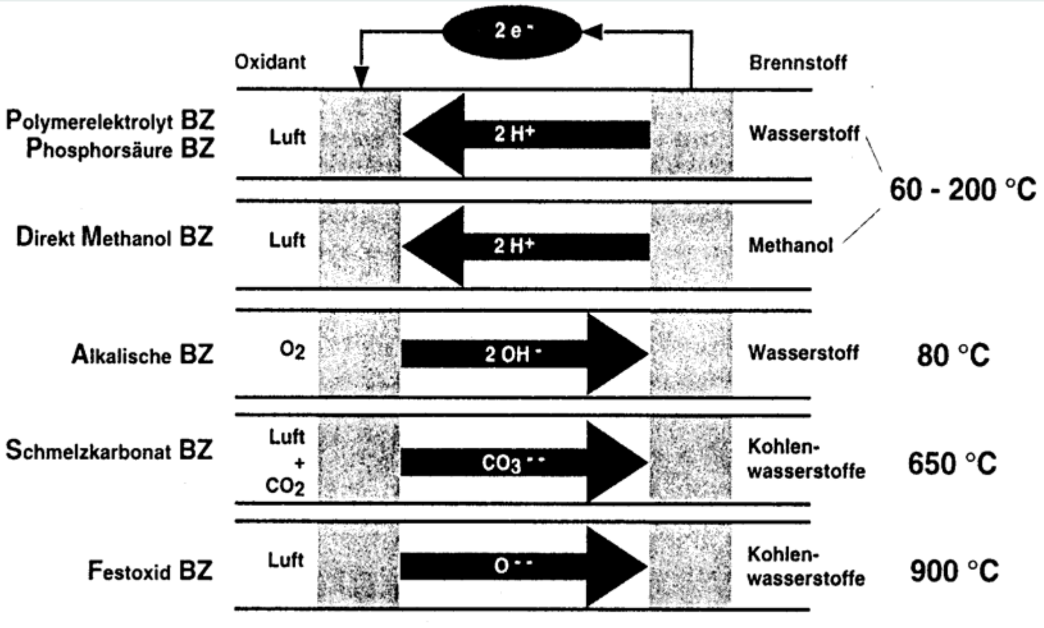

Next Generation Aerospace Material

R. NESPER ETH ZÜRICH & COLLEGIUM HELVETICUM

Carbon Nanotube

Nanotube Fiber

Nanotube/ Polymer

Ultra Nanostructured Composite

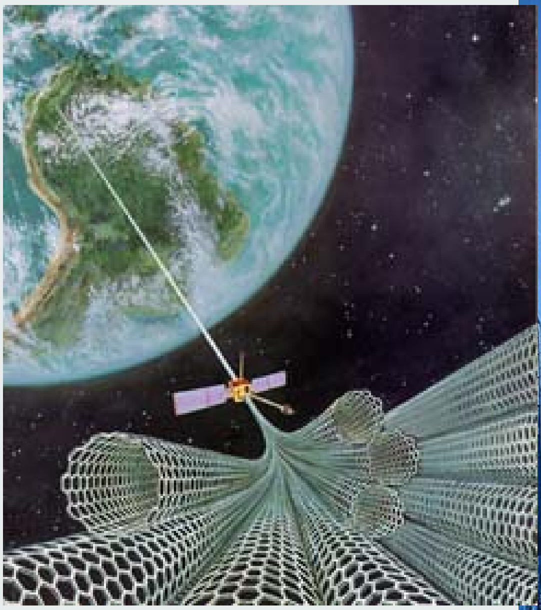

Self Similar Helical Modeling

R. NESPER ETH ZÜRICH & COLLEGIUM HELVETICUM

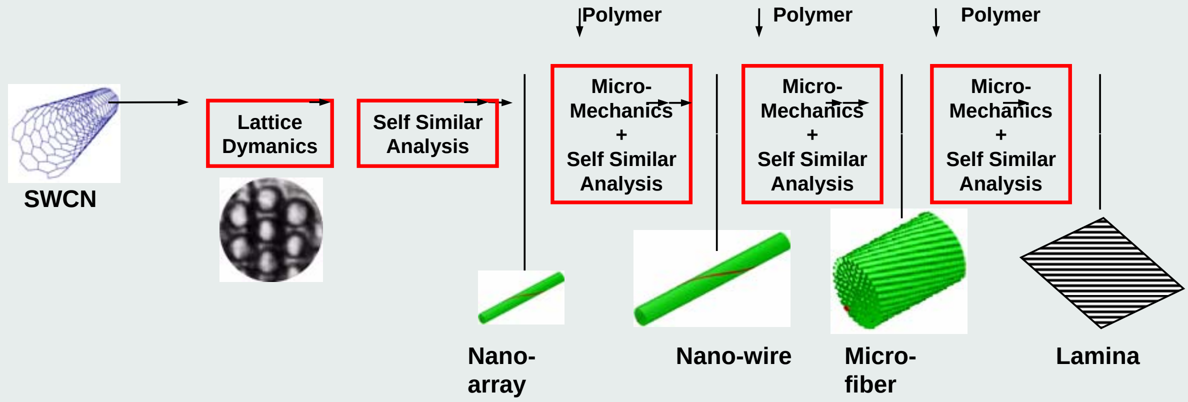

SWCN

Lattice Dymanics

Self Similar Analysis

Polymer

Micro-Mechanics + Self Similar Analysis

Polymer

Micro-Mechanics + Self Similar Analysis

Polymer

Micro-Mechanics + Self Similar Analysis

Nano-array

Nano-wire

Micro-fiber

Lamina

Self-Similar Scales

R. NESPER ETH ZÜRICH & COLLEGIUM HELVETICUM

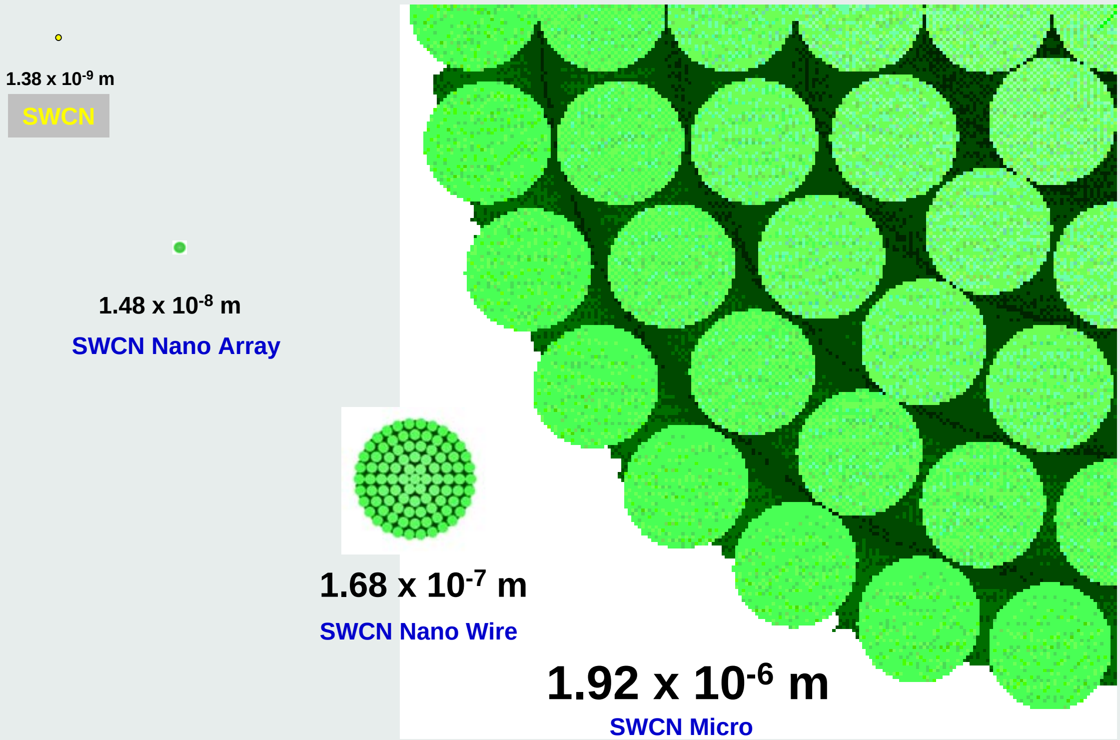

1.38×10^{-9} m

SWCN

1.48×10^{-8} m

SWCN Nano Array

1.68×10^{-7} m

SWCN Nano Wire

1.92×10^{-6} m

SWCN Micro Fiber

Self-Similar Scales

R. NESPER ETH ZÜRICH & COLLEGIUM HELVETICUM

Diameter = 1.92×10^{-6} m
Length = 1.0×10^{-3} m

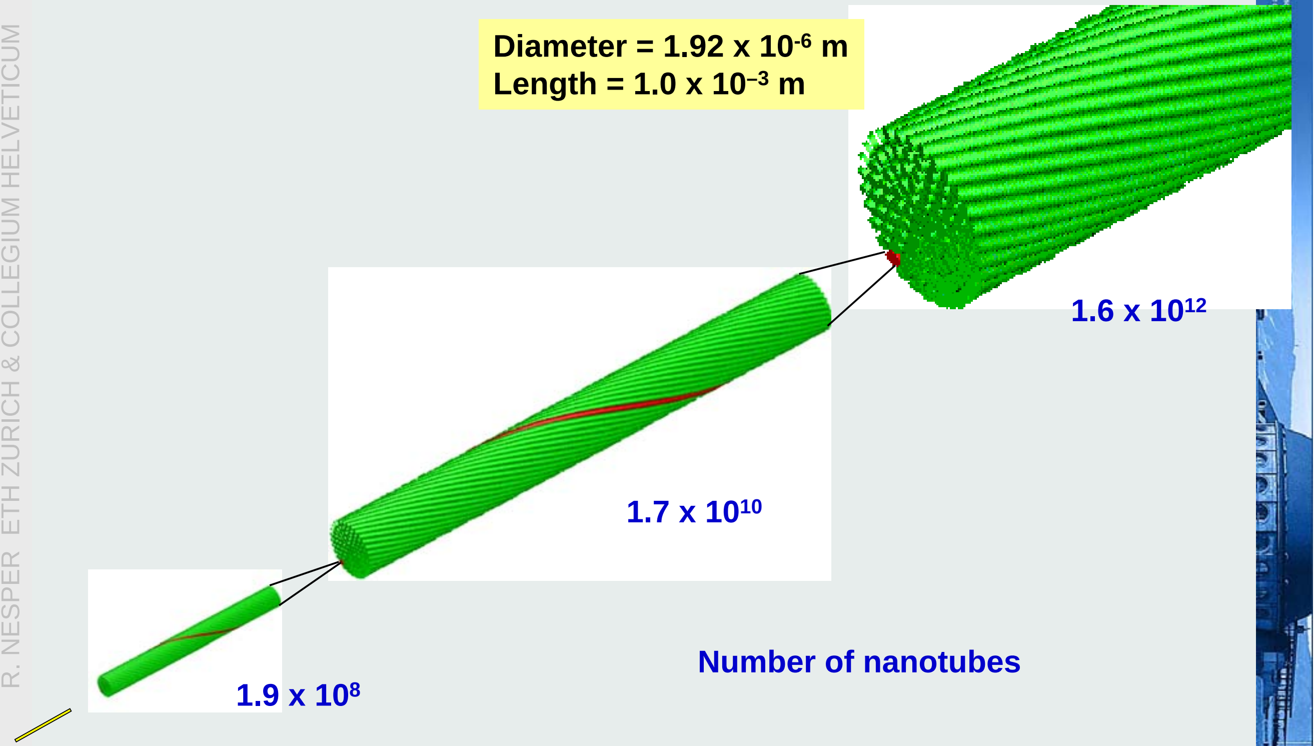

1.6×10^{12}

1.7×10^{10}

1.9×10^{8}

Number of nanotubes

SWCN

Self-Similar Properties